

Calibration and Characterization of a COTS Thermal Camera for Space

Abhilasha Jain
Department of Electronics
and Communication Engineering
Manipal Institute of Technology, Manipal
abhilashajain139@gmail.com

Dhananjay Sahoo
Department of Electronics
and Communication Engineering
Manipal Institute of Technology, Manipal
dhananjay.sahoo2296@gmail.com

Sarvani BSR
Department of Electronics
and Communication Engineering
Manipal Institute of Technology, Manipal
sarvani.seshasai@gmail.com

Sukumar K.
Department of Electronics
and Communication Engineering
Manipal Institute of Technology, Manipal
kai.sukumar@gmail.com

Ritvik Gupta
Department of Mechanical
and Manufacturing Engineering
Manipal Institute of Technology, Manipal
ritvikgupta95@gmail.com

Adheesh Boratkar
Department of Electronics
and Communication Engineering
Manipal Institute of Technology, Manipal
adheesh.boratkar@learner.manipal.edu

Abstract—This paper describes a progressive process for calibration of a shutter less Commercial off the Shelf (COTS) thermal imaging camera for small scale remote sensing applications. Usually thermal imagers are equipped with shutters which provide a uniform temperature source to correct the accumulated offset errors in the digital read outs of such cameras. This paper aims at radiometric calibration and compensatory correction methods for improved imaging via shutter less cameras. The thermal camera considered in this paper, consists of an uncooled micro-bolometer with a focal plane array of 640×512 pixels and field of view of 45×37 degrees. The foremost approach for calibration involved the use of a water bath, with nominal temperature control, placed in the Field of View of the camera. Following this, a different approach for calibration using a blackbody and temperature control for the camera was used. Using the Planck's Law, a relation was obtained between the digital number output from the Read out Integrated Circuit (ROIC) of the camera and the radiance of the black body. This equation allowed digital pixel value to be related to the temperature of the object being captured. Gain and offset maps for the entire FPA were obtained using this data.

payloads and fly them aboard self-made satellites. Due to the relatively small lifespans, Commercially-Off-The-Shelf (COTS) components are frequently used on board these satellites. These components however, have to be qualified and characterized to function in the space environment.

This paper focuses on the calibration and characterization of a COTS thermal camera to be used aboard a nanosatellite for remote sensing applications. The camera consists of an uncooled micro-bolometer with a focal plane array of 640×512 pixels and a field of view of 45×37 degrees. This camera lacks a shutter and hence this poses a major concern on accurate calibration. Furthermore, the camera is not intended for space use and required extensive testing. In order to fly this shutterless camera on a satellite, it also had to be calibrated actively. The paper describes a progressive approach employed to achieve calibration and characterization.

The content in the paper is divided as follows: Firstly, the camera is characterized for space use. Then a regression based calibration method is explained where commonly available equipment such as a water-bath is used. The limitations of this method are discussed and later the paper moves on to the calibration process involving black bodies. The improvements in the calibration of the camera using this method are explained. The paper concludes with results and the future scope of work in this regard.

TABLE OF CONTENTS

1. INTRODUCTION.....	1
2. CHARACTERIZATION OF THERMAL CAMERA FOR SPACE USE.....	1
3. REGRESSION BASED CHARACTERIZATION OF SENSOR	3
4. RADIOMETRIC CALIBRATION OF SENSOR.....	4
5. CONCLUSIONS AND FUTURE SCOPE	6
REFERENCES	6
BIOGRAPHY	6

1. INTRODUCTION

With the onset of small scale satellite projects such as micro, nano or pico-satellites, space has become a more accessible domain. The cost and complexity of a satellite has reduced enabling research groups and students to make their own

2. CHARACTERIZATION OF THERMAL CAMERA FOR SPACE USE

Before proceeding with the calibration of the thermal camera, it is important to ensure that the camera remains functional in space with no degradation in image quality. The thermal imager was tested in vacuum for performance degradation. It was placed in a vacuum chamber with a pressure of 10^{-5} bar for 48 hours as shown in Figure 1. The image quality was checked after the test and compared to the data taken before the test and the variance in the pixel value was found to be within permissible limits. The camera was also later powered on in vacuum to test operability. Outgassing was negligible and within limits specified by the ESA for space use [1]. The

camera also functioned as before.



Figure 1. Camera placed in a vacuum chamber.

The operating temperature of the camera is from -40°C to 80°C . The satellite on which the camera will be mounted has a passive method of temperature stabilization. By using thermal paints and tapes, the worst temperature cases inside the satellite were simulated. This was shown to be -19°C as the minimum and 41°C as the maximum. The simulations for the same are shown in Figure 2 and Figure 3 respectively. This was well within the operating temperature of the camera. Further, the electrical power system accounted for the use of an overcurrent/overvoltage protection circuit to prevent sudden surges from harming the camera. Hence with the clearance of vacuum and temperature requirements in space, the major focus shifted to the calibration of the camera which is explained in the subsequent sections.

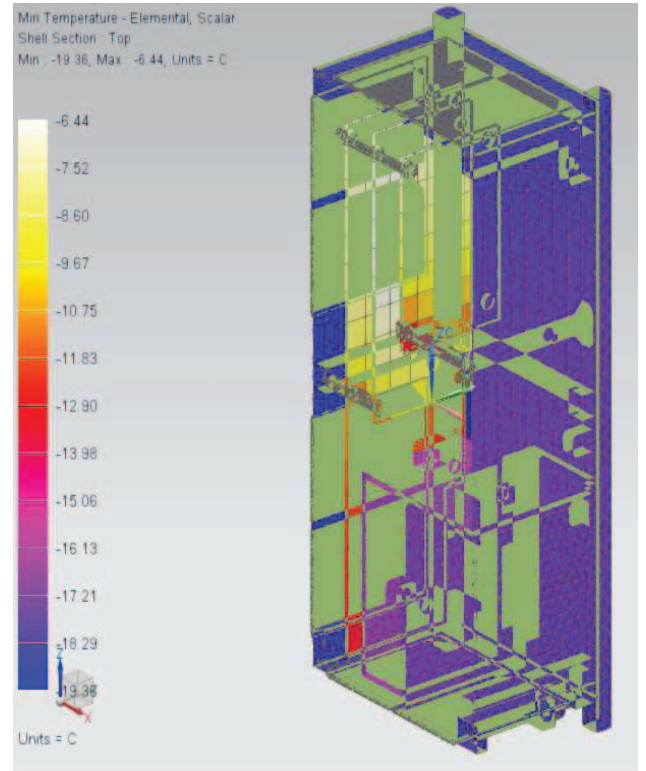


Figure 2. Minimum temperature simulation for satellite.

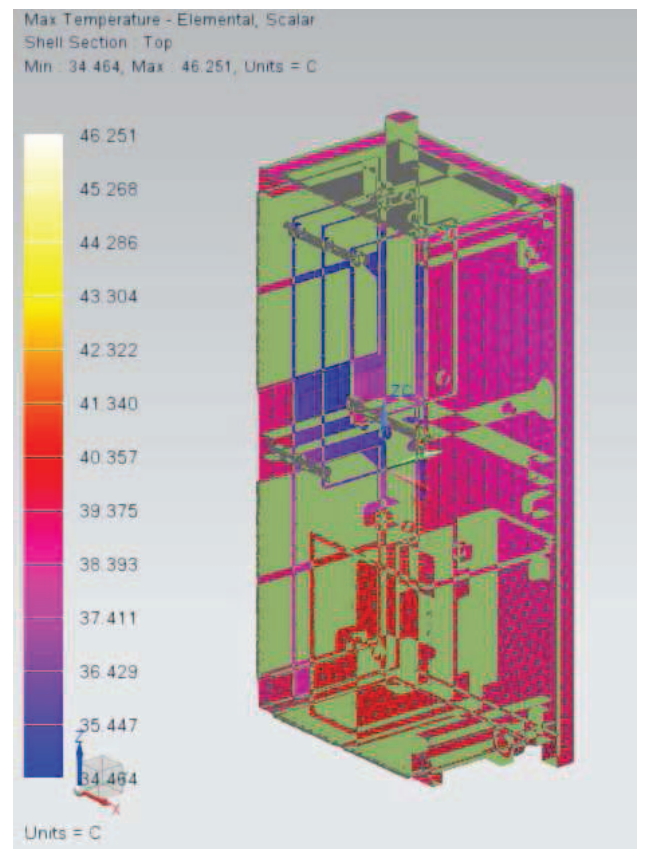


Figure 3. Maximum temperature simulation for satellite.

3. REGRESSION BASED CHARACTERIZATION OF SENSOR

The precursory approach for calibration involved the use of water bath, with nominal temperature control, placed in the Field of View(FOV) of the camera. The surface of the water was considered to be at a uniform temperature due to the presence of motor powered stirrers, which circulated the water, so as to maintain uniform temperature throughout the volume.

Flat fielding was done to compensate for different gains and offsets in the detector, after which a uniform signal creates a uniform output. This means that any further signal is due to the phenomenon being detected and not a systematic error. Hence, Flat field correction (FFC) is especially important to minimize or even remove sensor attributes and improve the image uniformity, as there are frequent performance discrepancies between pixels.

In the setup, the camera was clamped at some distance from the thermostat and was pointed towards the surface of water. The thermostat was set at a constant temperature and a set of images of the surface of the water were taken, with the FPA temperature varying. Before each image FFC was done using the Graphical User Interface (GUI) of the camera and, a body of uniform temperature was placed in front of the lens. This was done to enable correction of any non-uniformity in the Focal Plane Array (FPA).

FFC corrected the offset and gain of each pixel so as to get uniform readings of the water surface. We repeated this process for different scene temperatures from $30^{\circ}C$ to $50^{\circ}C$, with respect to varying FPA temperature. Throughout the experiment, it was ensured that the FOV of the camera was focused on the surface of water and not on the sides of the thermostat.

This was repeated for different materials for the purpose of doing FFC, i.e. white tile, cardboard and a metal sheet that was painted black.

The experiment was conducted at an ambient temperature of $30^{\circ}C$, and the minimum and maximum pixel value, mode, mean and variance of each image were calculated using MATLAB.

It was observed that the variance of Pixel value for the white tile was found to be higher than when the cardboard and black metal sheet was used.

Though the best data set was found for the black metal sheet it, did not make much of a difference when the regression model was calculated, since the mode of the pixel array was taken into account, at the time of formation of the regression model. The Images were analysed, and it was found that, the difference between mean and mode greater than 15, were discarded as the average difference was found out to be 11.66. Also images, with variance greater than 20 were not considered, as the average variance of the images was found to be 18.29. The above assumptions were taken, to remove any anomalous data, for the regression model.

Once the anomalies were removed, mathematical modelling was done, where sensor temperature, the gray pixel value and the scene (water bath) temperature were plotted to obtain a rough estimate to approximate an equation that could satisfy the data.

Figure 4 shows a 3D view of the plotted data with the following axes information:

- 1) X axis represents sensor temperature in $^{\circ}C$
- 2) Y axis represents numerical gray scale pixel value.
- 3) Z axis represents scene temperature in $^{\circ}C$.

Even after removing some of the anomalies from the data set, some stray points were still observed, which caused the least square error to increase. However, most of the data was near about a single plane.

A regression algorithm, specifically Marquardt-Levenberg gradient expansion algorithm was used to obtain an equation to satisfy the above data [2]. The following three two variable quadratic equation was found appropriate for regression:

$$z = p_1 + p_2x + p_3y + p_4x^2 + p_5y^2 + p_6xy \quad (1)$$

After regression the following values of the constants were obtained

$$\begin{aligned} p_1 &= -314.1370932 \\ p_2 &= -4.494235296 \\ p_3 &= 0.08198238437 \\ p_4 &= 0.04957069532 \\ p_5 &= -0.00000377895288 \\ p_6 &= 0.0002019237096 \end{aligned}$$

The plane formed by this equation along with the plotted data is shown in Figure 5.

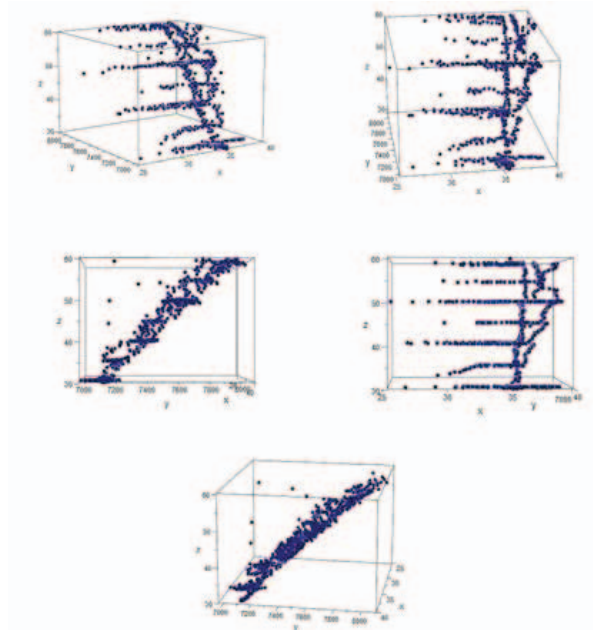


Figure 4. 3D plot of experimental data.

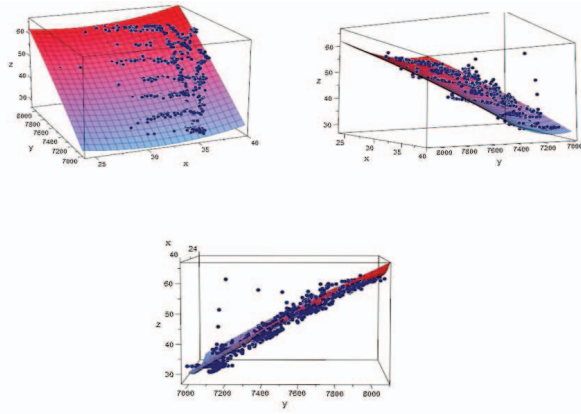


Figure 5. Plot of experimental data along with regression model .

The equation was tested on other images obtained later. The resultant temperature found by the equation deviated from the actual scene temperature. The method proved to be irregular and ineffective, possibly due to the following errors:

- Due to an absence of an internal shutter in the camera, an external body was used as a shutter. Hence, an angular error might have been present while keeping the body over the lens while doing FFC.
- Ripples were present on the surface of water due to the stirrer, which could have resulted in a distorted and hence an inaccurate image.
- Accuracy of the temperature sensor of the thermostat was limited due to its least count being 0.1°C , and hence the temperature of the sensor kept fluctuating.
- The effects of emissivity of water and atmospheric factors wasn't included.
- FFC, is a coarse way to deal with non-uniformity, it blemishes the details and, also enhances the noise locally in the images and reduces the effective dynamic range.

4. RADIOMETRIC CALIBRATION OF SENSOR

The quadratic approach to determine the object temperature was not feasible, as the polynomial was able to fit only a limited range of values and the accuracy of the results achieved by interpolation was low. The inaccuracies produced were mainly due to temperature noise, gain and offset of individual pixels [3]. Temperature noise is the unwanted temperature detected by the focal array, which includes the temperatures of the immediate environment of the camera, and also the FPA temperature itself. Gain of a pixel occurs due to manufacturing defects, such as different resistance values of similar pixels and is corrected to an extent at the factory. Offset/thermal drift is caused by the temperature variations of the Microbolometer, giving non-uniform temperature values, which continually varies over time. Offsets are commonly corrected using shutter-based method. Since a shutter less thermal camera is taken into consideration, other corrective methods are adopted, one of which is described in this paper. However, qualitative results can be achieved when both offset and gain are corrected, that is, two -point non-uniformity correction is employed.

Two-point non-uniformity correction includes obtaining the offset and gain errors for each pixel of the array and applying the corrective factors to an image for precise results. To calculate gain and offsets, the array is to be exposed to a uniform temperature source and hence, any differences in the pixel values are solely caused by these defects. A radiometric approach using a blackbody was adopted to obtain these maps. It was observed that a pixel value of the array was a linear function of the radiance incident on the bolometer array, which is given by Planck's equation, with gain as slope and offset as the intercept. The Planck's equation (with constants substituted) is given by:

$$L(\lambda, T) = \frac{c_1}{\lambda^5} \frac{1}{\exp(\frac{c_2}{\lambda T}) - 1} \quad (2)$$

Where,

L = incident radiance

λ = wavelength

T = scene temperature

$c_1 = 1.19104 \times 10^{-16}$

$c_2 = 1.438775 \times 10^{-5}$

And the digital pixel value is given by the equation:

$$\text{Pixelvalue} = a * L + b \quad (3)$$

Where,

L = incident radiance

a = gain

b = offset

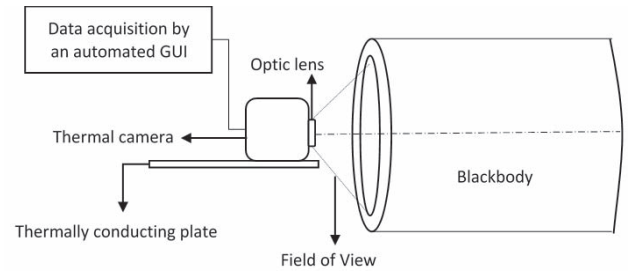


Figure 6. Block diagram of the experimental setup.

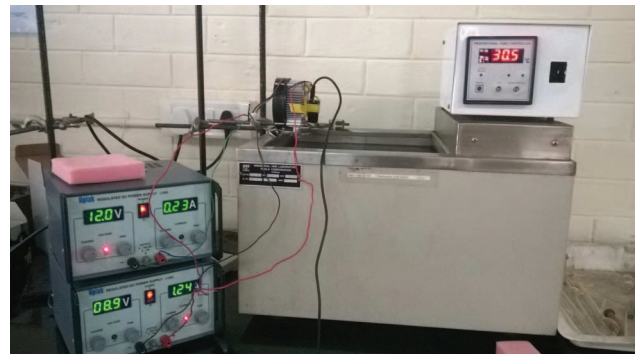


Figure 7. Test setup with temperature control.

The setup for radiometric calibration includes mounting the thermal camera on a good thermally conducting plate with

the help of a thermally conducting tape. The whole setup was maintained at a uniform ambient temperature of about 25°C and the conducting plate and the tape act as a heat sink, maintaining the bolometer array at a fairly constant temperature. Thus, the camera's sensor temperature was constant at 25°C throughout the experiment. The Field of View (FOV) of the camera is completely covered by a blackbody to ensure that all the pixels are exposed to a uniform temperature scene. The temperature of the blackbody was varied from 25°C to 50°C and a series of images were taken at every 5°C interval, while the data acquisition was done on an automated GUI.

From (3) we can write:

$$L = \frac{(Pixelvalue - b)}{a} \quad (4)$$

Equating (2) and (4), we get:

$$\frac{Pixelvalue - b}{a} = \frac{c_1}{\lambda^5} \frac{1}{\exp(\frac{c_2}{\lambda T}) - 1}$$

$$Pixelvalue = b + a * \frac{c_1}{\lambda^5} \frac{1}{\exp(\frac{c_2}{\lambda T}) - 1} \quad (5)$$

Equation (5) gives the relation between scene temperature and pixel value. Since LWIR (7.5μm – 13.5μm) radiation is being considered, a central wavelength of 10.5μm is taken as λ. The coefficients of the equation are taken as gain *a* and offset *b*.

To obtain the gain and offset values of each pixel of the array, numerical analysis method was employed. The temperature of the scene was taken on the X-axis, while the pixel values were taken on Y-axis and the data was fitted to the Equation (5), using the curve fitting tool of MATLAB.

MATLAB PSEUDO CODE:

1. *Create temperature array*
2. *Find mean values of pixels*
3. *For i from 1 to (640 * 512) do*
4. *Prepare data for curve fitting with temperature, mean as input*
5. *Fit curve to custom equation:*
6. $f(x) = b + \frac{(a * 1.19104 * 10^{-16})}{((10.5 * 10^6)^5 * (\exp(\frac{1.438775 * 10^{-5}}{10.5 * 10^{-6} * x}) - 1))}$
7. *Store a and b in gain and offset arrays*
8. *End do*

Thus, the coefficients, obtained had an R-square error of 0.9994 and the mean values of the data were:

Mean gain = $5.2572 * 10^{-08}$
Mean offset = $-3.4076 * 10^{+03}$

We observe that the gain and offsets are consistent with the Planck's law and also, the pixels possess similar gain and offsets, as was expected. But, the blackbody temperature was taken over limited temperature range with constant camera temperature. The maps can be applied to images within this range of scene temperature, for accurate results.

The resultant gain and offset maps were applied to a different set of images, taken at camera temperatures other than 25°C and the temperature were calculated by Equation (6).

$$T = \frac{c_2}{\lambda} \frac{1}{\ln(\frac{a * c_1}{\lambda^5 (pixelvalue - b)} + 1)} \quad (6)$$

However, when compared to the thermostat readings, the resultant temperatures were erroneous by a huge margin. Possible source of error could be that the FPA temperature of the new image set was different from the FPA temperature at the time of calibration. This is an important parameter as the biasing current flowing through the bolometer array, causes the FPA to heat up. This reduces the resistance of the array elements, affecting the array temperature and hence, the pixel value. As a remedy to control this parameter, a temperature controller for the camera is incorporated into the setup. The entire radiometric calibration procedure is repeated at different FPA temperatures. Thus, an extensive look-up table can be generated at different FPA temperatures, to obtain more qualitative and accurate results.

As it has been mentioned earlier also that the camera temperature and scene temperature were taken as the variables in the initial approach towards calibration and using regression and data sets an approximate function that correlated the digital number with the scene temperature and the camera temperature was obtained. However, the inaccuracy in that method was unpredictable and the method was scientifically not the best. Since camera temperature was taken to be a variable a plan to develop a mechanism to control the temperature of the camera had not been thought of. However, since the actual procedure of calibration has been understood and described as above, the temperature control of the mechanism is necessary as the temperature of the focal plane array of the camera also contributes to an error in the correlation of the digital number with the actual temperature of the scene or the target object. For this purpose, a temperature control setup shown in Fig 7. was proposed with the help of which the camera after heating up could be cooled down to any desired temperature by just giving the desired input. The basic principle of thermoelectric cooling was used [4]. (Thermoelectric cooling uses the Peltier effect and creates a heat flow between the junctions of two different types of materials).

The main principle behind the working of the Peltier cooler is the Peltier effect which is the inverse of the Seebeck effect. To understand the Peltier effect one first has to understand the Seebeck effect. In one line Seebeck effect can be described as the development of a potential difference across two dissimilar conductors or semiconductors held at different temperatures. At the atomic scale this can be explained by causing the charge carriers in the material to diffuse from the hot side to the cold side. The inverse of the Seebeck effect would be the generation of a temperature difference across two junctions by the application of a potential difference across them. The temperature difference generated across the surfaces depends upon the current flowing between the conductors, the Peltier

coefficients of the respective conductors and certain other factors like the heat flow between the two conductors due to the temperature gradient, heat flow between the surroundings and the surfaces. The set of Peltier coolers can be cascaded to generate the required temperature difference. Therefore, to cool a certain surface, it can be placed in contact with the surface of the cooler at the lower temperature and the surface of the cooler at the higher temperature can be placed in contact with the heat sink to constantly dissipate the heat gained and maintain the heat flow between the system and surroundings until the temperature reaches a constant.

The main components of the setup included a Peltier cooler [5] which could be controlled electronically and a cooling fan (heat sink) that was placed beside the cooler. The camera was placed in contact with the cooler and the fan was placed beside the entire setup as shown in the figure below. Both the Peltier cooler and the cooling fan were connected to DC voltage sources of 0-16V, 2A. The cooling fan had aluminium fins at its back side to allow for the passage of air through it and hence allowed for convection cooling of the hotter surface. The variation of the voltage connected across the cooler results in the variation of the temperature difference across its surfaces and the variation of the potential difference across the fan results in the variation of the speed of the fan. Varying the speed of the fan results in the variation of the rate of heat dissipation.

5. CONCLUSIONS AND FUTURE SCOPE

The paper demonstrated a basic calibration strategy using a water bath setup along with which regression analysis was used to find a polynomial relation between the system variables. However, this method could not be utilized for a wide range of temperatures that the camera may withstand while in orbit and produced wide error when the pixel values were interpolated back to the temperature using the same equation. We then moved to a more sophisticated approach utilizing a black body and a controlled thermal environment. The results obtained for this approach were far more useful for our study and could arrive at the temperature from the pixel value with an accuracy of ± 1 degree (when FPA temperature was constant). This test setup was refined, further by controlling the camera temperature using a thermoelectric Peltier cooler. Gain and offset maps using this refined setup gave a least square error of 0.998 as compared to an error of 0.001 obtained using the initial water bath setup. This ensured that temperature information of the objects was retrieved with an accuracy of 95. The calibration however was not complete, as the images obtained from the camera showed some pattern noise that arise due to a variety of reasons. In order to correct these errors, a Fourier domain approach was used. Hence, preliminary calibration using a black body and collection of correction algorithm at different sensor temperatures, fairly consistent error less images could be obtained. Through this paper, the authors hope to demonstrate a reliable method to use COTS hardware for space use.

REFERENCES

- [1] ESA ESMAT Outgassing requirements and database. www.esmat.esa.int/services/outgassing_data/outgassing_data.html
- [2] R. Olbrycht, B. Wiecek, New Approach to thermal drift correction and gain determination in Microbolometer thermal cameras, 12th International Conference on

Quantitative Infrared Thermography, 7-11.07.2014, Bordeaux, France.

- [3] Paul J. Thomasa, Alexander Savchenkoa, Peter Sinclair, Paulo Goldmana Richard Hornseyb, Canaan Hongb, Timothy Pope; Offset and gain compensation in an integrated bolometer array; SPIE Vol. 3698, pp. 826-836, July, 1999.
- [4] Disalvo, F. J. (1999). "Thermoelectric Cooling and Power Generation". Science 285 (5428): 7036. doi:10.1126/science.285.5428.703
- [5] STUDY OF THERMOELECTRIC COOLER Al-rubaye, A.T., Mousa, M.G., Hegazi, A.A.

BIOGRAPHY



Abhilasha Jain is a final year student of Manipal Institute of Technology, Manipal, India. She is pursuing her Bachelors degree in Electronics and Communication Engineering. She is the head of the Payload Subsystem of the university funded Student Satellite project. She has interest in computer architecture, embedded systems, and image processing.



Sukumar K. is a final year student of Manipal Institute of Technology, Manipal, India. He is pursuing his Bachelors degree in Electronics and Communication Engineering. He is heading the university funded satellite project as a systems engineer. His interests lie in system integration, computer vision and embedded design.



Dhananjay Sahoo is a junior at Manipal Institute of Technology Manipal, India. He is pursuing his Bachelors Degree in Electronics and Communication Engineering. He is a member of the Payload Subsystem. He is interested in electromagnetism, quantum physics and analog electronics.



Ritvik Gupta is a junior at Manipal Institute of Technology Manipal, India. He is pursuing his Bachelors Degree in Mechanical and Manufacturing Engineering. He is a member of the Payload Subsystem.



Sarvani B.S.R. is a junior at Manipal Institute of Technology Manipal, India. She is pursuing his Bachelors Degree in Electronics and Communication Engineering. She is a member of the Payload Subsystem Her interests include atmospheric science and applications of EMF in astronomy.



Adheesh Boratkar is currently working on avionics hardware development for TeamIndus, Indias only entry to the Google Lunar X-Prize. He has been involved with Manipal Universitys student satellite project, Parikshit since 2011. He has contributed towards the payloads of the satellite throughout and was leading the team as the lead systems engineer till May 2015 when he completed his Bachelors degree in Electronics and Communication Engineering. He continues to guide the team at the University.